Conformational Complexity in Seven-Membered Cyclic Triazepinone/Open Hydrazones. 1. 1D and 2D Variable Temperature NMR Study

Kalevi Pihlaja,* Mario F. Simeonov,† and Ferenc Fülöp‡

Department of Chemistry, University of Turku, FIN-20014 Turku, Finland

Received December 11, 1996⊗

The stereochemistry and conformational behavior of a series of 22 2-methyl-2-alkyl(phenyl, aryl)-4-*N*-methyl-1,2,3,4-tetrahydro-5*H*-1,3,4-benzotriazepin-5-ones and their open-chain hydrazone tautomers in various solvents were studied by 1D and 2D NMR techniques in the temperature range from 193 K to 410 K. Molecular rearrangements involving interconversions of the ring and open-chain forms (the latter via amide bond and *Z*/*E* C=N double bond isomerization), pseudorotation of the ring forms, and N-inversion processes with different rates on the NMR time scale took place, leading to the observation of average and deceptively simple ^{1}H and ^{13}C NMR spectra for most of them at room temperature.

Introduction

The therapeutic and commercial success of 1,4-benzodiazepines has stimulated considerable interest in related systems.[1] Since the biological activity is dependent on the stereochemistry of the seven-membered ring,[2] we were interested in studying a series of variably substituted 1,3,4-benzotriazepinones. Considerable confusion has surrounded the preparation[3] of these 1,4-benzodiazepine analogues due to the tautomeric process.[4] Many of the early benzotriazepinone structures were reassigned later as quinazolinones, imidazolines, oxadiazoles, and other structures,[3] *i.e.* the reactions of β-aminocarbohydrazides with oxo reagents can result in hydrazone, pyrimidinone, or triazepinone derivatives, depending on the substituents and the conditions employed.[5]

The first example of the formation of a seven-membered ring from an *o*-amino-substituted aromatic hydrazide was the reaction of anthranilic acid *N*,*N*′-dimethylhydrazide with carbonyl compounds.[5a] Later, the rearrangements of *o*-aminobenzoyl *N*-methylhydrazones of β-dicarbonyl[5b] and simple monocarbonyl[5c] compounds were shown by NMR spectroscopy to involve a ring/open-chain equilibrium in solution. *N*-Methyl carbohydrazides were observed to react with acetaldehyde, acetone, and cyclohexanone to yield cyclic products (condensed triazepinones), with benzaldehyde[5c] to yield open forms (hydrazones), and with acetophenone to yield a hydrazone benzotriazepinone ring/open-chain equilibrium, with tautomerism, in a 1:1 ratio (Scheme 1).

Scheme 1. Compounds Studied

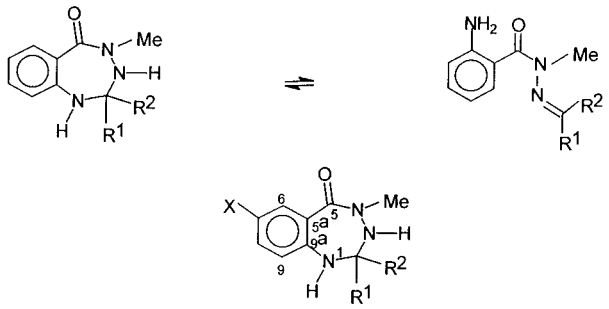

1 X = H, R^1 = Me, R^2 = Me
2 X = Cl, R^1 = Me, R^2 = Me
3 X = H, R^1 = Me, R^2 = *i*-Pr
4 X = H, R^1 = Me, R^2 = *t*-Bu
5 X = Cl, R^1 = Me, R^2 = *t*-Bu
6 X = H, R^1, R^2 = -$(CH_2)_5$-
7 X = H, R^1 = Me, R^2 = Ph
8 X = Cl, R^1 = Me, R^2 = Ph
9 X = H, R^1 = Me, R^2 = *p*-$NO_2C_6H_4$
10 X = Cl, R^1 = Me, R^2 = *p*-$NO_2C_6H_4$
11 X = H, R^1 = Me, R^2 = *p*-$CF_3C_6H_4$
12 X = Cl, R^1 = Me, R^2 = *p*-$CF_3C_6H_4$
13 X = H, R^1 = Me, R^2 = *m*-ClC_6H_4
14 X = Cl, R^1 = Me, R^2 = *m*-ClC_6H_4
15 X = H, R^1 = Me, R^2 = *p*-BrC_6H_4
16 X = Cl, R^1 = Me, R^2 = *p*-BrC_6H_4
17 X = H, R^1 = Me, R^2 = *p*-MeC_6H_4
18 X = Cl, R^1 = Me, R^2 = *p*-MeC_6H_4
19 X = H, R^1 = Me, R^2 = *p*-$MeOC_6H_4$
20 X = Cl, R^1 = Me, R^2 = *p*-$MeOC_6H_4$

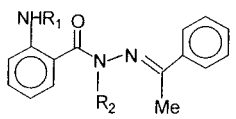

21 R_1 = H, R_2 = H
22 R_1 = Me, R_2 = Me

† Institute of Organic Chemistry with Center of Phytochemistry, Bulgarian Academy of Sciences, BG-1113 Sofia, Bulgaria.
‡ Institute of Pharmaceutical Chemistry, Albert Szent-Györgyi Medical University, H-6720 Szeged, POB 121, Hungary.

⊗ Abstract published in *Advance ACS Abstracts,* July 1, 1997.

(1) Bachman, G. B.; Levine, H. A. *J. Am. Chem. Soc.* **1947**, *69*, 2341.
(2) Fryer, R. I.; Cook, C.; Gilman, N. W.; Walser, A. *Life Sci.* **1986**, *39*, 1947
(3) (a) Sunder, S.; Peet, N. P.; Trepanier, D. L. *J. Org. Chem.* **1976**, *41*, 2732. (b) Peet, N. P.; Sunders, S. *J. Heterocycl. Chem.* **1984**, *21*, 1807. (c) Scheiner, P.; Frank, L.; Giusti, I.; Arwin, S.; Pearson, S. A.; Excellent, F.; Harper, A. P. *J. Heterocycl. Chem.* **1984**, *21*, 1817. (d) Leiby, R. W. *J. Heterocycl. Chem.* **1984**, *21*, 1825. (e) Peet, N. P. *Synthesis* **1984**, 1065. (f) Fülöp, F.; Simeonov, M.; Pihlaja, K. *Tetrahedron* **1992**, *48*, 531.
(4) Valters, R.; Fulöp, F.; Korbonits, D. *Adv. Heterocycl. Chem.* **1996**, *68*, 1.
(5) (a) Hromatka, O.; Knollmüller, M.; Krenmüller, F. *Monatsh. Chem.* **1969**, *100*, 941. (b) Gál, M.; Fehér, O.; Tihanyi, E.; Horváth, Gy.; Jerkovich, Gy. *Tetrahedron* **1982**, *38*, 2933. (c) Gál, M.; Tihanyi, E.; Dvortsak, P. *Acta Chim. Hung.* **1986**, *123*, 55. (d) Reddy, P. P.; Reddy, C. K.; Reddy, P. S. N. *Bull. Chem. Soc. Jpn.* **1986**, *59*, 1575.

S0022-3263(96)02322-5 CCC: $14.00

Table 1. ^{1}H and ^{13}C NMR Chemical Shifts[a] (ppm), Populations (%), and Thermodynamic Parameters (kcal mol^{-1}) of Compound 1

	δ, 293 K		δ, 273 K		δ, 233 K
nucleus	ring form	open form	ring form	open form	ring form
(C-2)-CH_3	1.37[b] (27.2)	1.84[b] (19.6)	1.29[b] (nd)	1.84[b] (nd)	1.20 (27.0)
(C-2)-CH_3	1.37[b] (27.2)	2.06[b] (24.9)	1.40[b] (nd)	2.06[b] (nd)	1.45 (26.7)
(N-4)-CH_3	3.30 (38.8)	3.23 (nd)[c]	3.27 (nd)	3.27 (nd)	3.29 (38.6)
(N-1)-H	4.48	4.48	4.54	4.54	4.60
(N-3)-H	3.73[b]	–	3.90[b]	–	4.00[b]
population	98	2	99	1	100
$\Delta\Delta G°_{(ring \rightleftharpoons open)}$	2.3		>2.5		
$\Delta\Delta G°_{(ring\ dynamic\ process)}$			13.0		
other nuclei					
C-2	(77.4)	(nd)	(nd)		(77.6)
C-5	(172.7)	(161.7)	(nd)		(172.7)

[a] The latter in parentheses. [b] Signal broadening. [c] nd = not detected.

Factors such as *N*-substitution, ring-closure, possibility of conjugation, and steric hindrance have been found to govern the equilibria.[5c] Thus, it is evident that, like other seven-membered benzoheterocyclic compounds,[4] the substituted benzotriazepines are extremely complex and rather flexible systems. Not surprisingly, therefore, little is known about the conformations attained by these systems in solution.[6a] Actually, only a few examples of 1,3-*N*,*N*-heterocycles showing ring/open-chain tautomerism are known.[4,6b–d]

The primary goal of this work was to determine the structure in solution of the studied compounds. However, a detailed conformational analysis was required due to the wealth of dynamic chemistry that embodies not only the ring/open-chain rearrangement, but also the interconversions of the ring and open-chain forms (the latter via an amide bond and *Z*/*E* C=N double bond isomerism), pseudorotation of the ring, and N-inversion proceeding with different rates on the NMR time scale, but leading to the average and deceptively simple ^{1}H and ^{13}C NMR spectra at room temperature.

All these findings impelled us to set two goals for this initial work: (i) by means of 1D and 2D NMR studies at variable temperatures, to characterize the complex conformational properties of compounds **1**–**22** (Scheme 1) in different solvents (this work); and (ii) to relate the NMR thermodynamic parameters to molecular model calculations and X-ray measurements in order to gain additional insight into the dynamic processes in these seven-membered benzoheterocycles (Part 2[6e]). A detailed computational study of the open-chain hydrazone forms found for most of the compounds will be reported elsewhere.

Results and Discussion

Compounds 1–6. Ring Forms. The ^{1}H and ^{13}C NMR chemical shifts of **1** and **2**–**4** are listed in Tables 1 and 2, respectively. The cross-peaks observed in the 2D HETCORR and 2D LR HETCORR NMR spectra were crucial for the complete assignment of the spectra. Further, the special changes occurring upon change of the solvent and during thermal activation permitted assignment of the different sets of peaks up to three [one ring (R) and two open-chain (O1 and O2)] forms.

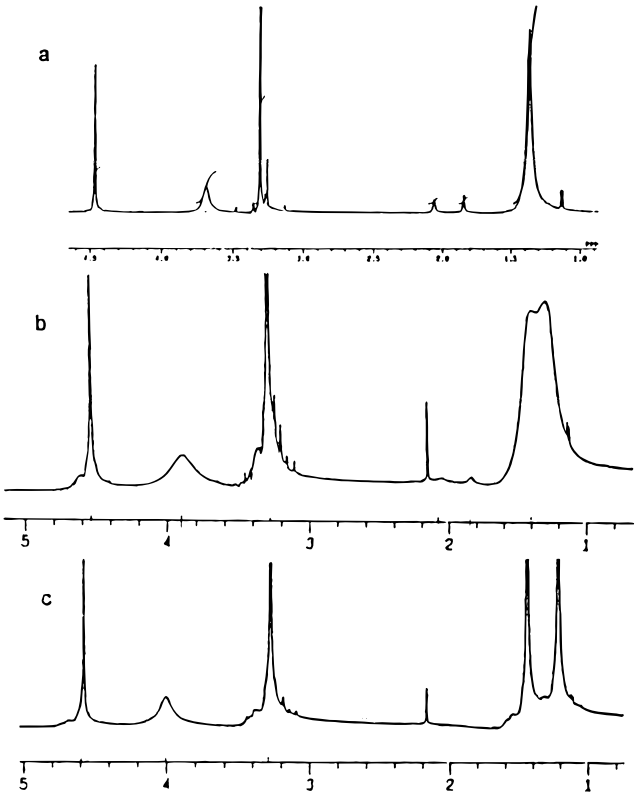

Figure 1. ^{1}H NMR spectra of **1** in CD_2Cl_2 at (a) 293, (b) 273, and (c) 233 K.

In CD_2Cl_2 at room temperature (293 K), **1** is present in two forms: R and O1. Crucial parts of the ^{1}H NMR spectrum of **1** at different temperatures are shown in Figure 1. The spectrum at 293 K exhibits broad signals at 1.37 and 3.73 ppm, corresponding to the (C-2)-methyl protons and (N-3)-H proton of the ring form, respectively. The former peak correlates with the peak at 77.4 ppm (C-2) in the 2D LR HETCORR spectrum at 293 K. The ^{13}C spectrum (Figure 2a) also reveals some weak signals due to the open form, *e.g.* C-2 in this form in **2**–**4** resonates at *ca.* 170 ppm (see Table 2; the NMR parameters for **5** and **6** are very close to those of compound **4**). Further, the ^{1}H NMR signals of **1** at 3.30 and 3.23 ppm were assigned to the (N-4)-methyl protons of the R and O1 isomers, respectively. The signal at 3.30 ppm has cross-peaks with the carbon resonances at 38.8 (in the 2D HETCORR spectrum) and 172.7 ppm (in the 2D LR HETCORR spectrum), assigned to the (N-4)-methyl and C-5 of the ring form, respectively. The ^{1}H and ^{13}C NMR

(6) (a) Messinger, J.; Buss, V. *J. Org. Chem.* **1992**, *57*, 3320. (b) Korbonits, D.; Tobiás-Héja, E.; Kolonits, P. *Chem. Ber.* **1991**, *124*, 1199. (c) Korbonits, D.; Tobiás-Héja, E.; Simon, K.; Kolonits, P. *Chem. Ber.* **1991**, *124*, 2065. (d) Lambert, J. B.; Wang, G.; Huseland, D. E.; Takiff, L. C. *J. Org. Chem.* **1987**, *52*, 68. (e) Simeonov, M. F.; Fülöp, F.; Sillanpää, R.; Pihlaja, K. *J. Org. Chem.* **1997**, 62, 5089.

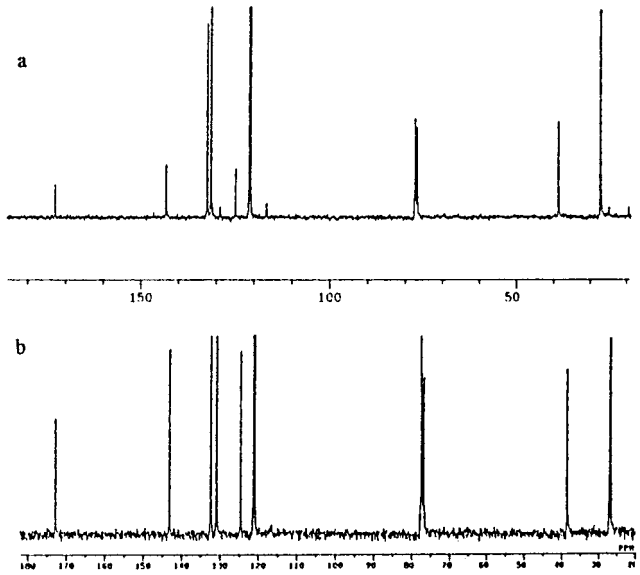

Figure 2. ^{13}C NMR spectra of **1** in CD_2Cl_2 at (a) 293 and (b) 233 K.

data for the ring conformer of **1** agree closely with those observed by Gál *et al.*[7] All conformational energy differences ($\Delta G°$) between the ring and open-chain forms were estimated from the integrals (I) of the (N-4)-methyl and/or (C-2)-methyl protons, using the equation $\Delta G° = -RT \ln K$, where $K = I$(major form)/I(minor form)[8] for **1**−**4** (see Tables 1 and 2).

When a CD_2Cl_2 solution of **1** is cooled, the ^{13}C NMR spectrum at 233 K (Figure 2b) reveals only one set (R-form) of carbon signals. Now two peaks relating to the (C-2)-methyl carbon, at 27.0 ppm and 26.7 ppm, and a strong C-2 resonance at 77.6 ppm are observed. In the ^1H spectra of **1** at 273 K and 233 K (Figure 1b,c), the peak at 1.37 ppm is split into a doublet (1.20 ppm and 1.45 ppm), whereas the signal of the (N-3)-H protons at 4.00 ppm is still a broad singlet. Thus, within the temperature range examined, three dynamic processes occur in **1**: (i) a rapid ring interconversion affecting mainly N-3 and C-2 and the respective methyl groups with an energy barrier ($\Delta G^‡$ value, calculated via the coalescence temperature method[8]) of *ca.* 13.0 kcal mol^{-1} at $T_c = 273$ K and freezing out at 233 K; (ii) ring/open-chain rearrangement with $\Delta G^‡$ higher than 13.0 kcal mol^{-1} and with a Gibbs energy difference ($\Delta G°$) of 2.3 kcal mol^{-1} in favor of the ring form; and (iii) a rapid (on the NMR time scale) N-3 nitrogen inversion process with a $\Delta G^‡$ less than 13.0 kcal mol^{-1}.

Nearly the same ^1H and ^{13}C NMR chemical shifts as those for **1** were observed for **2**, except for the downfield shifted C-2 signal (of the ring form) by *ca.* 10 ppm. The latter must be due to the electron-withdrawing effect of the chlorine atom on C-7, an evidence for the *para*−*para* interaction in the (C-9a)−(N-1)−(C-2) moiety, as suggested by the X-ray results and molecular modeling. The ring/open and open/open molecular rearrangements of **2** appear to be much slower than those of **1**, since the proportion of the open form was still increasing after a week, and peaks corresponding to other open forms were also appearing [mainly for the (N-4)-methyl protons; see Table 2].

Table 2. ^1H and ^{13}C NMR Chemical Shifts[a] (ppm), Populations (%), and Thermodynamic Parameters (kcal mol^{-1}) of Compounds 2−4

	2		**3**		**4**		
nucleus	ring (R) form	open (O1) form	ring (R) form	open (O1) form	open (O2) form	ring (R) form	open (O1) form	open (O2) form
(C-2)-CH_3	1.37[b] (27.3)	1.80 (19.6)	1.20[b] (19.4)	1.90[b] (15.3)	2.12 (20.0)	1.34 (20.5)	1.77[b] (14.1)	2.15 (24.5)
(C-2)-R	1.37[b] (27.2)	2.08 (24.9)	1.01, 1.03 (17.7)	1.07, 1.10 (17.0)	1.15[b] (17.8)	1.03 (25.6, 39.5)	1.05[b] (27.3, 39.0)	1.17 (26.2, nd)
			1.70 (36.8)	2.54 (35.8)	(nd)[f] (36.5)			
(N-4)-CH_3	3.30 (39.0)	3.26[c] (nd)	3.25 (38.5[d])	3.22 (40.0)	3.20 (41.5)	3.30[b] (39.2)	3.26 (40.0)	3.24 (nd)
(N-1)-H	4.40	4.40	4.40	4.38[b]	4.38[b]	4.69	4.62[b]	4.42[b]
(N-3)-H	3.70[b]	–	4.38[b]	–	–	4.55[b]	–	–
population	90	10	70 (62[e])	23 (29[e])	7 (9[e])	21 (15[e])	67 (85[e])	12 (0[e])
$\Delta\Delta G°_{(ring\rightarrow open)}$	1.3		0.6 (0.4[e])	0.7 (0.7[e])		−0.7 (−1.0[e])	1.0 (2.6[e])	
other nuclei								
C-2	(87.0)	(nd)	(82.0)	(167.0)	(nd)	(82.4)	(166.9)	(170.0)
C-5	(171.5)	(nd)	(172.7[e])	(181.6)	(nd)	(172.6)	(183.4)	(182.8)

[a] The latter in parentheses. [b] Signal broadening. [c] Three signals (δ 3.25 (6%), δ 3.34 (4%), and δ 3.21 (2%)) after four days. [d] Cross-peak with δ 3.25 in 2D LR HETCORR spectrum. [e] At 323 K. [f] nd = not detected.

(7) Gál, M.; Pallagi, I.; Sohár, P.; Fülöp, F.; Kálmán, A. *Tetrahedron* **1989**, *45*, 3513.
(8) Rahman, Atta-ur. *Nuclear Magnetic Resonance, Basic Principles*; Springer Verlag: New York, 1985.

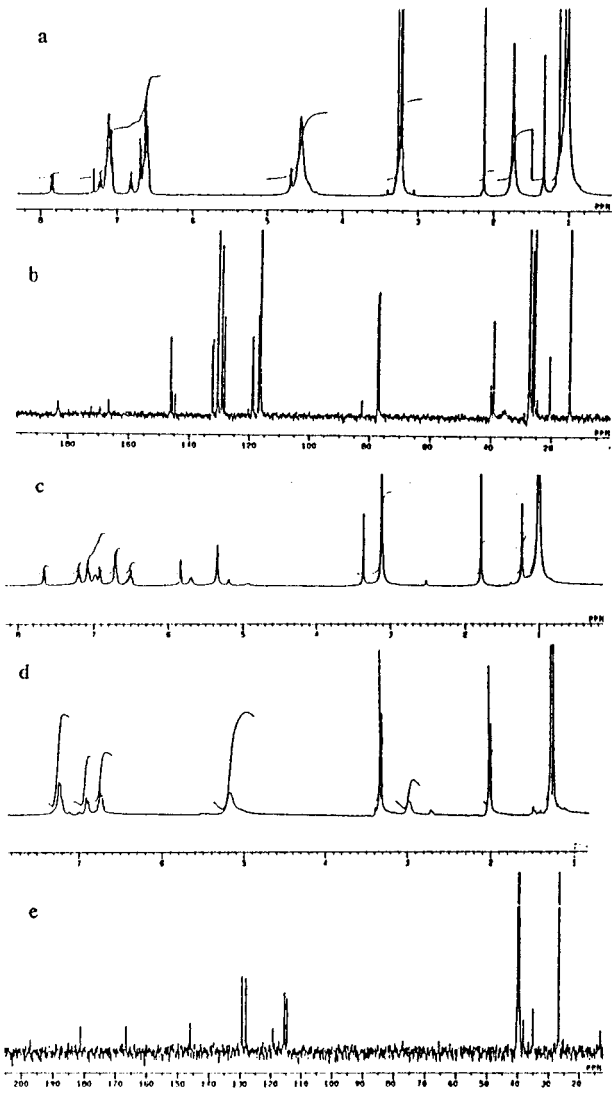

Figure 3. ^{1}H and ^{13}C NMR spectra as a function of solvent and temperature for **4**: (a) ^{1}H NMR spectrum in $CDCl_3$ at 293 K, (b) ^{13}C NMR spectrum in $CDCl_3$ at 293 K; (c) ^{1}H NMR spectrum in DMSO-d_6 at 293 K; (d) ^{1}H NMR spectrum in DMSO-d_6 at 433 K; (e) ^{13}C NMR spectrum in DMSO-d_6 at 433 K.

The ^{1}H and ^{13}C NMR spectra of **3** and **4** are rather complex. They were interpreted in terms of a superposition of three subspectra corresponding to one ring and two open forms, the latter being favored for **4** (see Table 2). The ^{1}H and ^{13}C NMR spectra for **4** are shown in Figure 3. The complete assignment was achieved through analysis of the 2D HETCORR and 2D LR HETCORR NMR spectra. A similar broadening as for **1** was observed, *i.e.* the same dynamic processes must occur in **3** and **4.** An upfield shift of the (C-2)-methyl carbon signal occurred, from *ca.* 27 ppm in **1** to *ca.* 20 ppm in **3** and **4**, which must be due to the well-known steric compression shift effect[9,10] of the bulky substituents in **3** and **4**. A similar shift was not observed for the (N-4)-methyl carbon. Thus, it may be concluded that the favored ring form of **3** and **4** in solution is an inverted boat, with the (C-2)-methyl group orientated between the (N-4)-methyl and the bulky alkyl groups. Our 1D ^{1}H NOE difference measurements on **4** show that (i) irradiation of the *tert*-butyl protons (at 1.03−1.05 ppm, ring/open forms) gives NOE (14%) at 1.77 ppm [(C-2)-methyl protons, O1 form, see below) and some effects at 7.19 and 6.54 ppm (aromatic H-8 and H-9 of the ring form, respectively), but not at the (N-4)-methyl protons, in agreement with the inverted boat form, and (ii) irradiation of the ring (C-2)-methyl protons at 1.34 ppm gives NOE at 3.30 ppm [(N-4)-methyl protons of the ring form] and on the *tert*-butyl protons in agreement with the above assumptions.

On increase of the temperature from 293 to 323 K the population of the ring form of **3** decreased from *ca.* 70% to 62%, mainly at the expense of the major open form. Heating a sample of **4** in DMSO-d_6 caused more drastic changes in the population ratios, and only one set of signals for open forms was detected at 433 K (cf. Table 2).

As for **2**, the time-dependent ^{1}H NMR spectrum of **4** provides an insight into the thermodynamic features of the ring/open-chain equilibria: initially, the ring/open-chain ratio is *ca.* 1:4; after a week, the peaks of the open form became broad; later, peaks due to the second open-chain form were detected. Thus, one can speculate that in the crystalline state **4** attains the open form, that the energy barrier of the ring/open-chain interconversion of this compound is less than that between the open forms, and that the latter in turn is less than the energy needed for the ring transformation. Similarly, it can be estimated that the energy barriers of the ring/open-chain and ring-inversion processes for **4** are higher than those for **1**−**3**. The observed difference (*ca.* 1.5 kcal mol) between the values of $\Delta G°$ (ring/open) for **1** and **3**, and for **3** and **4**, can be explained simply by the change in the total nonbonded through-space methyl/methyl interactions on going from **1** to **3**, and from **3** to **4**.

For **5**, a small change in the ring/open-chain ratio was observed, which can be attributed to the electronic effect of the (C-7)-chlorine, as in the case of **2**. The NMR spectral parameters of **6** are similar to those for **1** (*i.e.* the conformational behavior is related), besides the fact that no signal broadening was found, except that of the (N-3)-H proton, due to a nitrogen-inversion process.

Open-Chain Forms (hydrazones). As mentioned above, one or two sets of signals relating to open forms were observed in the ^{1}H and ^{13}C NMR spectra of **1**−**4**. The assigned chemical shifts of these isomers are given in Tables 1 and 2. C-2, which resonates at *ca.* 80 ppm in the ring form, is deshielded to *ca.* 165 ppm in the open-chain hydrazones. The chemical shifts of the (C-2)-azomethine carbon of hydrazones are known to be between ca. 150 ppm and 180 ppm,[10] while those for the hydrazones of aliphatic aldehydes and alicyclic ketones are *ca* 180 ppm and those for the corresponding aromatic aldehydes *ca* 150 ppm.[11] In some pyruvate hydrazones, the greater electron-withdrawing power of pyruvate as compared with that of aryl groups causes additional upfield shifts to *ca.* 140 ppm.[12] The same effect has been observed in some arylaldehyde *N,N*-dialkylhydrazones.[13]

Two sets of ^{1}H and ^{13}C chemical shifts were observed for the (C-2)-methyl group in the hydrazones of **1**−6

(9) Grant, D. M.; Cheney, B. V. *J. Am. Chem. Soc.* **1967**, *89*, 5315.
(10) Breitmaier, E.; Voelter, W. *NMR Spectroscopy*; Verlag Chemie: Weinheim, 1974. Kalinowksi, H.; Berger, S.; Braun, S. *NMR Spektroscopie*; Georg Thieme Verlag: Stuttgart, New York, 1984. Pihlaja, K.; Kleinpeter, E. *Carbon-13 NMR Chemical Shifts in Structural and Stereochemical Analysis*; VCH Publishers, Inc.; New York, 1994.
(11) Fülöp, F.; Semega, É.; Bernáth, G.; Sohár, P. *J. Heterocycl. Chem.* **1990**, *27*, 957.
(12) Palla, G.; Predieri, G.; Domiano, P.: Vignali, C.; Turner, W. *Tetrahedron* **1986**, *42*, 3649.
(13) Brehme, R.; Radeglia, R.; Gründemann, E. *J. Prakt. Chem.* **1990**, *332*, 911. Brehme, R. *Chem. Ber.* **1990**, *123*, 2039. Brehme, R.; Klemann, A. *Tetrahedron* **1987**, *43*, 4113.

Scheme 2

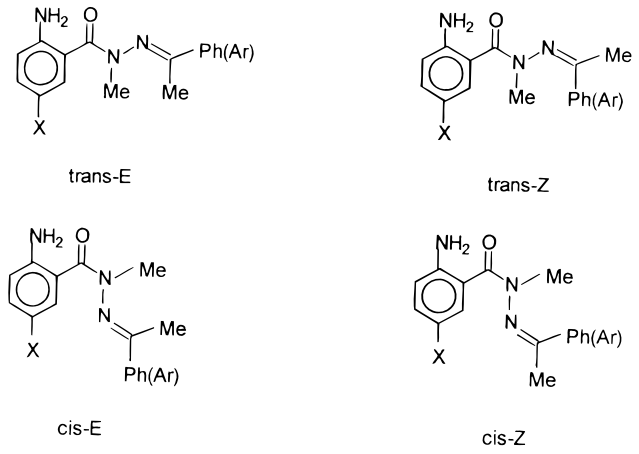

(Tables 1 and 2): (i) at *ca.* 1.8 and *ca.* 20 ppm, respectively (at higher field in the cases of **3** and **4**), for the major form (O1); and (ii) at *ca.* 2.2 and *ca.* 24 ppm, respectively, for the minor form (O2). Similar values were observed by Palla *et al.*[12] for some *N*-acyl- and *N*-aroylhydrazones. In principle, two *Z*/*E* geometrical isomers and two *cis*/*trans*-amide conformers can be found for the studied hydrazones as concerns the azomethine double bond and amide bond isomerism, respectively (Scheme 2).

For **1**, it is reasonable to assign the ^{1}H and ^{13}C chemical shifts of 1.84 and 19.6 ppm, respectively, to the (C-2)-methyl group closer to the (N-4)-methyl protons and thus upfield shifted due to the steric compression shift, *i.e.* γ-gauche effect.[9,10] Thus, the major open-chain form (O1) in **3**−**6** corresponds to the *E* isomer and the minor form (O2) to the *Z* isomer.

Additionally, the literature data[12] show that the benzoylhydrazone of methyl pyruvate, both in DMSO-d_6 and in $CDCl_3$, prefers the *trans*-amide conformer, as in the solid state. Our NMR data also suggest that in the open forms the rotation around the (C-5)−(C-5a) bond is hindered by the intramolecular H-bond of type N−H···O(C) as evidenced by the upfield chemical shift of the phenyl proton in the *ortho* position to the carbonyl group, whereas in the ring forms of **1**−**20** these signals appear at *ca.* 7.8 ppm, separately from the multiplet of the other aromatic protons at 6.6−7.3 ppm.

The question of the preference of a *trans*- or *cis*-amide structure as a consequence of *N*-methylation is quite interesting and remains open for some compounds.[14] Our 1D ^{1}H NOE difference measurements on **4**, immediately after dissolution, when the O1 form predominates (see above), show a strong (*ca.* 36%) NOE effect at 7.16 ppm and *ca.* 7% NOE at 6.67 ppm (aromatic H-6 and H-7, respectively, in an open form) when the N-methyl protons are irradiated. This result supports the *trans*-amide bond arrangement in O1.

All the above experimental findings prompt us to believe that the hydrazones of **1**−**6** are (i) in a *trans*-amide configuration in the crystalline state and in solution; (ii) the thermal, time- and solvent-induced open-chain isomerization of **1**−**6** discussed above involves their *Z*/*E* transformation. The literature data show that the energy barrier for this process is *ca.* 25 kcal mol^{-1} in some *N*-acyl- and *N*-aroylhydrazones[12] and *ca.* 23 kcal mol^{-1} in some *N*,*N*-dimethyl- and diphenylhydrazones,[15] which are high as compared to our observations on the time-dependent changes in **2**−**6**: the signal broadening for the (C-2)- and (N-4)-methyl protons in CD_2Cl_2 at room temperature, and the calculated energy barrier of *ca.* 18 kcal mol^{-1} for **4** in DMSO-d_6 at 323 K. On the other hand, Palla *et al.*[12] showed that the electronic effects can change the energy barriers of the *cis*/*trans*-amide bond and/or *Z*/*E* processes, depending on the substituents (see the discussion below). Because of the lack of definite ^{1}H and ^{13}C NMR evidence for the structural assignment in solution [*e.g.* from the chemical shifts of the (N-4)-methyl and (C-2)-methyl groups in the different isomers] and because of the conformationally relevant NOE values, which can be misleading in case of molecular equilibrations which proceed at rates fast on the NMR scale,[16] our considerations should also be treated with some caution. In order to investigate the *cis*/*trans* and *Z*/*E* preferences, and also the phenomenon of N−N rotation as a function of structure, MM and semiempirical MO calculations are in progress for these and other model compounds.

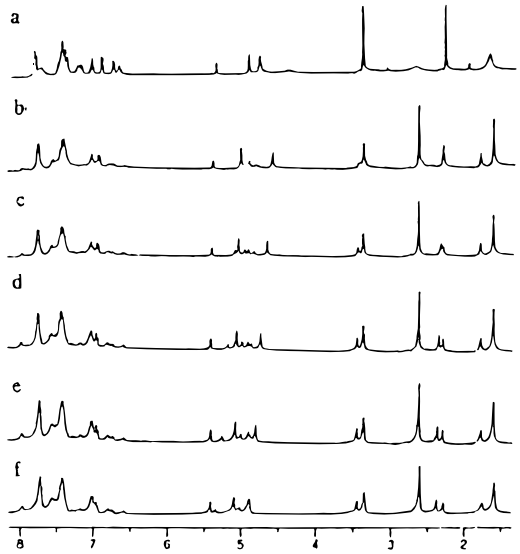

Figure 4. ^{1}H NMR spectrum of **7** in CD_2Cl_2 at (a) 293, (b) 273, (c) 253, (d) 233, (e) 213, and (f) 193 K.

Compound 7. This compound belongs in the series (**7**−**20**) with a phenyl or aryl group at C-2. At room temperature, all these molecules seem to be even more flexible than **1**−**6** and to undergo the same complex rearrangement as discussed above for **1**−**6**. Therefore, a detailed ^{1}H and ^{13}C NMR study of **7** was undertaken in the temperature range from 190 K to 390 K in CD_2Cl_2 and DMSO-d_6 as solvents, and time-dependent spectra were also recorded.

Immediately after dissolution, the ^{1}H and ^{13}C NMR spectra of **7** at 293 K can be interpreted in terms of two superimposed subspectra corresponding to (i) averaged broad and weak signals of the ring forms and (ii) another set of sharper peaks relating to the open-chain isomer(s) (Figures 4a and 5a, respectively) and in a *ca.* 1:1 ratio. Comparison of the ^{1}H spectrum of **7** with those of **1**−**6** led to the postulation that the broad peak at 2.7 ppm belongs to the (N-4)-methyl protons of the ring form, which therefore seem to be located in the shielding cone of the (C-2)-benzene ring. Thus, the most upfield, broad

(14) Itai, A.; Toriumi, Y.; Saito, S.; Kagechika, H.; Shudo, K. *J. Am. Chem. Soc.* **1992**, *114*, 10649.

(15) Shvo, Y.; Nahlieli, A. *Tetrahedron Lett.* **1970**, 4273.

(16) Kessler, H.; Griesinger, C.; Lautz, J.; Müller, A.; van Gunsteren, W. F.; Berendsen, H. J. C. *J. Am. Chem. Soc.* **1988**, *110*, 3393.

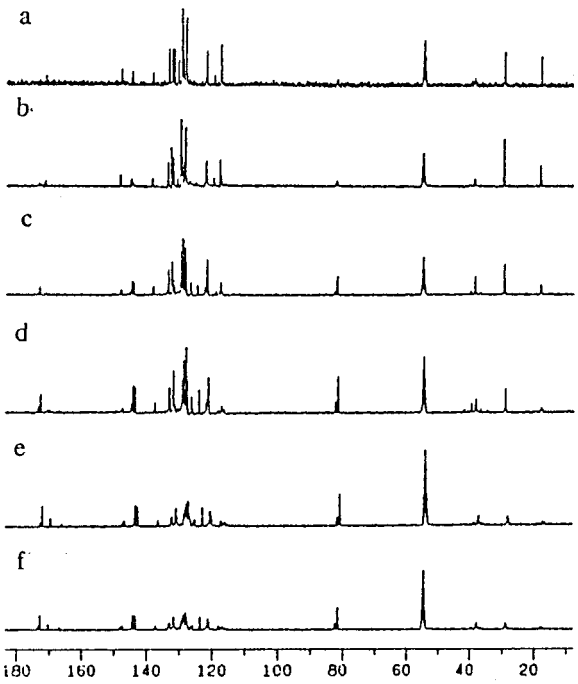

Figure 5. ^{13}C NMR spectrum of **7** in CD_2Cl_2 at (a) 293, (b) 273, (c) 253, (d) 233, (e) 213, and (f) 193 K.

Table 3. ^1H and ^{13}C NMR Chemical Shifts[a] (ppm) of Compound 7 in $CDCl_3$ at 293 K

nucleus	ring form	open form
(C-2)-CH_3	1.70[b] (28.6[b])	2.26 (17.1)
(N-4)-CH_3	2.70[b] (37.9[b])	3.38 (37.9[b])
(N-1)-H	4.70[b]	4.80
(N-3)-H	4.20[b]	–
C-2	(81.2)	(170.5)
C-5	(172.4)	(168.0)
C-5a	(128.3)	(118.2)
HC-6	7.84 (131.7)	7.22 (129.4)
HC-7	7.03 (121.2)	6.65 (116.6)
HC-8	7.33 (132.5)	7.15 (131.1)
HC-9	6.80 (120.8)	6.70 (116.8)
C-9a	(143.2)	(146.8)
C-1′	(131.8)	(137.2)
HC-2′,6′	7.30 (128.4)	7.30 (128.0)
HC-3′,5′	7.70 (127.1)	7.75 (127.1)
HC-4′	7.40 (130.7)	7.40 (130.7)

[a] The latter in parentheses. [b] Signal broadening.

signal at 1.7 ppm is due to the (C-2)-methyl protons of the ring form(s). The second set of two sharper signals in the aliphatic region, at 2.26 and 3.4 ppm, were assigned to the (C-2)- and (N-4)-methyl protons of the open-chain form(s), respectively. The ^{13}C spectrum confirms this assumption. The peaks at 17.1 and 28.6 ppm relate to the (C-2)-methyl carbons of the open-chain and ring forms, respectively; the broad and weak peak at 37.9 ppm can be assigned to the (N-4)-methyl carbon, and the weak signal at 81.2 ppm to C-2 of the ring form. Complete assignment of these deceptively simple and averaged ^1H and ^{13}C spectra was achieved by means of a combined use of 2D HETCORR and 2D LR HETCORR spectra optimized for the three-bond *trans* H/C configuration [*i.e.* for $J(H,C) = 12.5$ Hz]. Thus, the cross-peaks at 28.6/1.7 ppm and 17.1/2.3 ppm in the 2D HETCORR spectrum, and those at 170.5/2.3, 137.2/7.3, and 137.2/2.3 ppm in the 2D LR HETCORR spectrum were used to distinguish the two sets of peaks relating to the ring and open-chain forms (see Table 3). The observed ^1H and ^{13}C NMR chemical shifts of the (C-2)- and (N-4)-methyl groups reveal that the open-chain form is O1 (*trans*-E). The full ^1H and ^{13}C NMR assignments of **7** in CD_2Cl_2 at 293 K are given in Table 4.

At low temperature (see Figures 4b–f and 5b–f), both the ^1H and ^{13}C NMR spectra exhibit more complex patterns. Thus, on cooling to 273 K, the broad peaks at 2.7 and 4.2 ppm [(N-3)-H] were first sharpened and shifted downfield (*i.e.* N-inversion becomes slower) and the peak at 1.7 ppm was split into two singlets (1.62 and 1.79 ppm). Additionally, a peak appeared at 3.46 ppm, due to the (N-4)-methyl protons not located in the shielding cone of the (C-2)-aryl group. The coalescence of this ring inversion process occurred near room temperature, and the energy of activation was calculated to be *ca.* 14.7 kcal mol^{-1}. On further cooling to below 253 K, a clear splitting of the signals at 2.3 and 3.4 ppm occurred, due to the freezing of the interconversion of the open-chain forms to *trans-E* (O1) and *cis-E* (O2), as confirmed by the ^{13}C spectra (see below), and the energy of activation was calculated to be *ca.* 12.8 kcal mol^{-1} (T_c = 253 K). These conclusions were also consistent with the relative intensities observed for the two subspectra of the ring and open-chain isomers: the changes in peak intensity at 1.7 ppm are reflected in the peak intensity at 2.7 ppm, and those at 2.3 ppm in the peak intensity at 3.4 ppm.

In the ^{13}C NMR spectrum of **7** at 253 K, two sets of peaks corresponding to the two ring conformations were distinguished, the most characteristic of them being those at 28.1 ppm [(C-2)-methyl carbon], 37.5 ppm and 39.0 ppm [(N-4)-methyl carbon], 81.1 ppm and 81.9 ppm (C-2), 142.6 ppm and 143.4 ppm (C-9a) (see Table 4). Further, at 233 K the ring forms gave two more signals, at 172.1 ppm and 172.2 ppm (C-5), whereas the peaks of the open forms, after some broadening at 253 K (near coalescence), started to split at this and lower temperatures: the C-2 signal at 170.1 and 169.7 ppm (233 K); the C-9a signal at 146.7 and 147.0 ppm (233 K); the *N*-methyl carbon at 35.9 and 41.0 ppm (233 K); the (C-2)-methyl carbon at 17.1 ppm split into two peaks (16.5 and 17.2 ppm) at 213 K, *etc.* (see Table 4). Below 213 K, the peaks at 167.0 and 168.5 ppm were assigned to C-5 in the open forms, *i.e.* they are shifted about 10 ppm upfield in comparison with those for the open forms of **1**–**6**.

The results from the 2D HETCORR and the optimized 2D LR HETCORR experiments at 193 K were also consistent with our conclusions. Thus, in the 2D HETCORR spectrum the cross-peaks at 2.7/37.3 ppm [(N-4)-CH_3, R1 form] were now observed, and in the 2D LR HETCORR spectrum the following cross-peaks via two, three, and four bonds were detected: 1.6/81.2 ppm [(C-2)-CH_3/C-2, R1], 5.0/142.6 ppm [(N-1)-H/C-9a, R1], 4.8/123.0 ppm [(N-1)-H/C-5a, R2], 6.8/123.0 ppm (H-9/C-5a, R2), 2.3/169.9 ppm [(C-2)-CH_3/C-2, O1], 7.3/142.6 ppm (H-8/C-9a, R1), 1.6/142.6 ppm [(C-2)-CH_3/C-9a, R1], and 1.8/143.4 ppm [(C-2)-CH_3/C-9a, R2]. The latter two cross-peaks, which may be due to a four-bond W-arrangement of the (C-9a)–(N-1)–(C-2)-CH_3 moiety, are consistent with the boat and inverted boat forms of **7**, but not with the chair form. These results were further considered in connection with our molecular modeling of **7**.[6e]

An inspection of Dreiding models shows that the upfield shifts of the (C-2)-methyl protons from 1.79 and 1.62 ppm at 273 K to 1.66 ppm and 1.50 ppm at 192 K, and of the (N-4)-methyl protons from 2.66 to 2.51 ppm, and the downfield shifts of the N-1 and N-3 protons to 5.3 and 4.7 ppm, respectively, can be explained by the proposed ring conformation in which the benzene ring

Table 4. ^{1}H and ^{13}C NMR Chemical Shifts[a] (ppm), Populations (%), and Thermodynamic Parameters (kcal mol^{-1}) of Compound 7 under Different Conditions[b]

nucleus	ring (R1)[c] form	ring (R2)[c] form	ring (R3)[c] form	open (O1)[e] form *trans-E*	open (O2)[e] form *cis-E*	open (O3)[d] form *trans-Z*	open (O4)[d] form *cis-Z*
(C-2)-CH_3	1.62 (28.2)	1.79 (28.1)	1.37 (27.2)	2.20 (16.5)	2.17 (20.0)	2.62 (26.6)	2.38 (27.2)
(N-4)-CH_3	2.70 (37.5)	3.46 (39.0)	3.30 (38.8)	3.46 (37.9[f])	3.46 (37.9[f])	3.24 (37.9[f])	3.10 (37.9[f])
(N-1)-H	5.0	4.8		4.9			
(N-3)-H	4.1	4.6		–	–	–	–
population	28[d]		17[d]	26[d]		28[d]	
$\Delta G^{\ddagger}$ for dynamic processes	14.7 (293 K)			12.8 (253 K)			
other nuclei[c]							
C-2	(81.1)	(81.9)		(170.1)	(169.7)		
C-5	(172.1)	(172.2)		(167.0)	(168.5)		
C-9a	(142.6)	(143.4)		(146.7)	(147.0)		

[a] The latter in parentheses. [b] See the notes. [c] At 273 K and below. [d] Close to the equilibrium state (after a month). [e] At 253 K and below. [f] Splits at 233 K as follows: δ 37.2, 37.3, 35.9, 38.7, and 41.0.

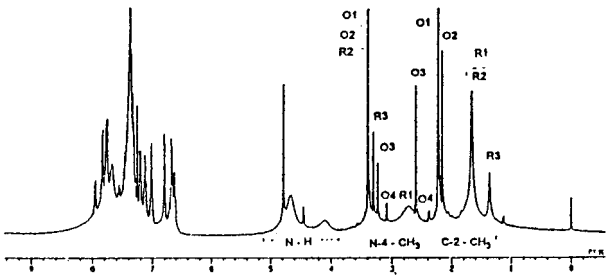

Figure 6. ^{1}H NMR spectrum of **7** at near equilibrium state (after a period of 1 month) in $CDCl_3$ at 293 K.

rotation around the (C-2)−(C-2′) bond can affect the above chemical shifts via the ring current effects.

Thus, at room temperature, fast rearrangements take place including pseudorotation of the boat to the inverted boat form, with exclusive predominance of the former. However, the time-dependent changes observed mainly in the ^{1}H NMR spectra of **7** within a period of more than a month showed clearly that other, much slower rearrangements also occurred between the ring form, the ring and open forms, and the open forms themselves. At first, a third ring form (R3) appears, giving peaks at 1.37 ppm for the (C-2)-methyl protons and at 3.30 ppm for the (N-4)-methyl protons with a population of *ca.* 17%, whereas the population of the (R1 + R2) forms decreases to *ca.* 28%. As it concerns the open forms, up to four forms were observed: after the appearance of different sets of peaks for O1 (27%), O2 (14%), O3 (7%), and O4 traces (see Figure 6), the amount of O2 decreases to traces, and at a near equilibrium state the population of O1 is *ca.* 26% and that of O3 is *ca.* 28%. The principal ^{1}H and ^{13}C NMR chemical shifts of all detected forms of **7** and the calculated conformational free energy differences between them are listed in Table 4. Thus, whereas the pair of open-chain isomers in **3** and **4** were assigned as *trans-Z,E*, O1 and O2 in **7** are *trans-E* and *cis-E* isomers [δ-(C-2)-methyl carbon *ca.* 17 ppm) and the O3 and O4 forms must be assigned as *Z* isomers [δ(C-2)-methyl carbons *ca.* 27 ppm), *i.e.* the former signals are shifted to a higher field due to the γ-gauche effect[9,10] (already discussed above), a consistently reliable criterion[10] (see Scheme 2).

To further clarify the thermodynamics of these rearrangements of **7**, we ran ^{1}H and ^{13}C NMR spectra at higher than room temperature in DMSO-d_6 solution. The reversibility of the spectral changes was confirmed. As in $CDCl_3$, two sets of signals were found in the spectra up to 353 K, and on further heating up to 413 K the peaks of O1 (*ca.* 57%), O3 (*ca.* 10%), and the ring form (*ca.* 33%) were observed. Hence, the thermal (noncatalyzed) activation of the isomerization of **7** in a polar solvent shows that the barrier height for the *E*/*Z* (O1−O3) interconversion around the C=N bond is not reached until 423 K (the coalescence region was not observed), but some increase in the O3 form population was experienced, and thus the *trans-E*/*trans-Z* transformation occurs via the *cis-E* form. Moreover, the standard Gibbs energy differences between the open forms O1, O2, and O3 calculated from the populations close to the equilibrium state at room temperature (see Table 4) were found to be near zero. Thus, the dynamic process seems to be under kinetic control, opposite to what was observed for **1**−**6**, where the energy of activation for the *Z*/*E* transformation is lower (this transformation is slow at room temperature and does not occur via any *cis*-amide form), but the conformational energy differences are higher. As to the energy of activation of *E*/*Z* as compared to *cis*/*trans*-amide bond transformations, the situation with **7** is again opposite to that with **1**−**6**. Below the room temperature, **1** was found only in the ring form, whereas **7** undergoes *trans-E*/*cis-E* transformation, with $\Delta G^{\ddagger}$ of *ca.* 12.8 kcal mol^{-1} at T_c = 253 K, *i.e.* lower than in the case of **1**−**6**. A higher barrier for *Z,E* (*ca.* 21−24 kcal mol^{-1}) than for the amide bond (ca. 14−17 kcal mol^{-1}) isomerization in some aroylhydrazones of methyl pyruvate has been reported and explained in terms of electronic effects.[12] Hence, in our compounds the replacement of a (C-2)-alkyl by a phenyl group causes visible changes in thermodynamic behavior, due to the different electronic and steric properties of the substituents. An indication of such an effect is, *e.g.*, the about 10 ppm upfield shift of the C-5 resonance in **7**−**20** as compared with **1**−**6**. As mentioned above, MM and semiempirical MO calculations are in progress on the open-chain isomers of these and other model compounds and will provide a detailed insight into the problem.

While the thermodynamic behavior of the open forms of **7** can be explained mainly in terms of changes in their electronic properties relative to **1**−**6**, the conformational behavior of the ring form(s) of **7** mainly reflects the steric effect of the phenyl substituent.

Compounds 8−20. It was of interest to inspect the influence of substituents with different electron-withdrawing or -releasing powers on the phenyl ring(s) of **8**−**20** upon the rearrangement processes described above

Scheme 3

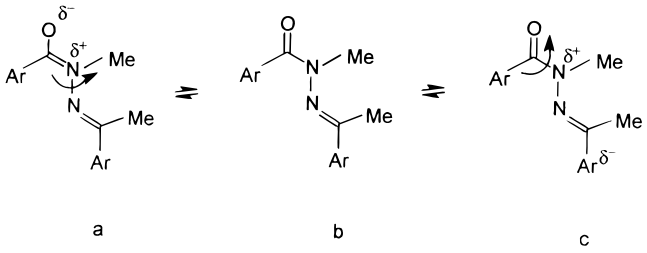

for **7**. Such an effect may be attributed only to the differences in their electronic properties, *i.e.* to resonance effects and electrostatic interactions obeying the classical picture of the forces that control conformational preference.[17]

The ^{1}H and ^{13}C NMR spectral assignments and hence the structure determination of **8**−**20** were achieved on the basis of those of **7**, as well as from the time (a few weeks)-dependent changes in their spectra at room temperature, assisted by 2D NMR experiments (*e.g.* **19**).

As for **7**, the initial state of the complex equilibrium favors the ring boat (R1 and R2) form(s) in rapid exchange and the *trans-E* open-chain isomer, but the relative amounts of these forms vary essentially with the substitution in **8**−**20**. The dynamic processes observed were an interconversion (i) of the open-chain *trans-E* (O1) to the *cis-E* (O2), *trans-Z* (O3), and boat forms, and (ii) of the latter to the N-3-inverted (B)′ form [*i.e.* (R3)] form, giving a new O1/R1 ratio in the equilibrium state. A temporary increase in the amount of the O2 isomer, as for **7**, was observed in most cases. Moreover, the rate of interconversion in the above processes obviously increases when going from **9** to **20**. Compounds **9**−**16**, bearing electron-withdrawing groups (EWG), display a higher rate of interconversion and a greater amount of O2 and a lower amount of O3 forms at equilibrium state, *i.e.* an easier amide-bond and a more difficult C═N rotation than in **7** and **17**−**20**. Thus, the electronic factors controlling the conformational behavior of the open-chain forms of **7** were strengthened in the case of **8**−**20**. In comparison with **1**−**6**, phenyl and/or EWG groups at the azomethine carbon in our hydrazones lead to a barrier-lowering effect for the *cis*−*trans* amide bond rotation, and to a barrier-raising effect for the *Z*/*E*-transformation process, and both observations can be explained in terms of electronic effects (Scheme 3).

As to the ring forms, an initial preference of R1 over O1 (ratio *ca.* 2:1) and the absence of the R3 conformer were noted for **9**−**16**. Only for **9** and **10** two different ring forms with δ(C-2)-methyl protons at 1.68 and 1.57 ppm were observed, just after dissolution, and were assigned to the boat and inverted boat forms. Hence, the barrier-raising effect of the *p*-NO_2 group was observed for the ring-flipping process in **9** and **10**, in comparison with **7** and **11**−**20**. In general, a reduction in the electron-withdrawing power and an increase in the electron-releasing power of the substituents when going from **9** to **20** favor the (*N*-3)-inverted boat (R3) form, the amount of which increases, whereas that of R1 drastically decreases. An essential difference in the populations of the ring and open forms was also observed when the effect of the chlorine substituent on the benzo part of the benzodiazepine ring was considered. Thus, for the counterparts **11**/**12** and **13**/**14**, the chlorine substituent causes an increase in the R3 population at the expense of R1; and for the counterparts **9**/**10** an increase in the O2 population at the expense of O1.

Although conjugation clearly exerts some effect on the barriers to rotation in **7**−**20** (Scheme 3), the complexity of the observed ring/open-chain rearrangement processes makes a quantitative study in terms of a simple linear correlation: $\log K_x = \rho\sigma^+ + c$, where K_x = [ring]/[chain], found valid in our previous comparative studies of 2-aryltetrahydro-1,3-oxazines[18] and 1,3-oxazolidines,[19] impossible.

Experimental Section

NMR Spectra. The 1D and 2D NMR spectra were measured on a JEOL JNM GX-400 spectrometer operating at 399.78 MHz for ^{1}H and 100.53 MHz for ^{13}C, respectively, using a 5 mm ^{1}H/^{13}C dual probe head (90° ^{1}H rf pulse width, 16 ms; 90° ^{13}C rf pulse width, 8 ms; 90° decoupler rf pulse width 40 ms). All chemical shifts were referenced to the solvent [δ = 7.24 and 77.1 ppm ($CDCl_3$), δ = 2.49 and 39.5 ppm (DMSO-d_6), and δ = 5.32 and 53.8 ppm (CD_2Cl_2) for ^{1}H and ^{13}C, respectively]. The digital resolution of the 1D NMR spectra was 0.2 and 0.7 Hz per point for ^{1}H and ^{13}C, respectively. JEOL automatic microprograms were applied to obtain DEPT, ^{1}H NOE difference spectra, 2D HETCORR, and 2D LR HETCORR NMR spectra. The ^{1}H NOE difference spectra were acquired with a pulse width of 8 ms, a duration of irradiation of 1000 ms, and a delay of relaxation of 8 s. The 2D experiments normally involved a 128 × 2 K data matrix with NS = 640 and NE = 64. In 2D HETCORR and 2D LR HETCORR experiments, delays of 3.33 and 2.22 ms, and 40 and 20 ms were used to optimize the sensitivity for the response of the direct and long-range ^{1}H/^{13}C coupling constants, respectively. After zero filling in F1, a sine-bell nonshifted weighting was used in both dimensions. The spectrometer was fitted with a variable-temperature accessory capable of maintaining temperature to within ±2 K.

Syntheses. The crystalline 1-(2′-aminobenzoyl)-1-methylhydrazines and the 5′-chloro derivative were prepared according to a literature[20] method, starting from the corresponding isatoic anhydrides with methylhydrazines. The aldehydes and ketones used were commercial products. Melting points were determined on an Electrothermal digital melting point apparatus and are uncorrected.

A. Reactions of 1-(2′-Aminobenzoyl)-1-methylhydrazines with Aliphatic Ketones. A mixture of 1-(2′-aminobenzoyl)-1-methylhydrazine or 1-(2′-amino-5′-chlorobenzoyl)-1-methylhydrazine (2 mmol) and 5 mL of a ketone (acetone, 3-methyl-2-butanone and 3,3-dimethyl-2-butanone were used) was refluxed for 4−20 h. The reaction was monitored by means of TLC. After evaporation of the solvent, products **1**−**5** crystallized out on ethereal treatment. The yields were 56−67%.

B. Reaction of 1-(2′-Aminobenzoyl)-1-methylhydrazines with Cyclohexanone. 1-(2′-Aminobenzoyl)-1-methylhydrazine (1 mmol) was dissolved in 5 mL of 50% ethanol, and 0.5 g of cyclohexanone was added. The product started to crystallize out after a few min. After standing overnight, **6** was filtered off and recrystallized from 50% EtOH in 84% yield.

C. Reactions of 1-(2′-Aminobenzoyl)-1-methylhydrazines with Acetophenones. A mixture of 1-(2′-aminobenzoyl)-1-methylhydrazine or 1-(2′-amino-5′-chlorobenzoyl)-1-methylhydrazine (2 mmol), an acetophenone derivative (2 mmol), and *p*-toluenesulfonic acid (10 mg) was refluxed in benzene (15 mL) for 5−8 h. The solvent was evaporated off, and products **7**−**20** crystallized out after ethereal treatment and were recrystallized. The yields were 70−90%.

(17) Riddell, F. G. *The Conformational Analysis of Heterocyclic Compounds*; Academic Press: 1980; p 7.

(18) Fülöp, F.; Pihlaja, K.; Mattinen, J.; Bernáth, G. *J. Org. Chem.* **1987**, *52*, 3821.

(19) (a) Fülöp, F.; Bernáth, G.; Mattinen, J.; Pihlaja, K. *Tetrahedron* **1989**, *45*, 4317. (b) Fülöp, F.; Pihlaja, K.; Neuvonen, K.; Bernáth, G.; Argay, Gy.; Kálmán, A. *J. Org. Chem.* **1993**, *58*, 1967.

(20) Fülöp, F.; Pihlaja, K. *Org. Prep. Proc. Int.* **1991**, *23*, 377.

Table 5. Analytical Data on 2,2-Disubstituted-1,2,3,4-tetrahydro-5*H*-1,3,4-benzotriazepin-5-ones 1−20

						anal. calcd/found, %		
no.	R^1	R^2	X	mp (°C) solvent	formula MW	C	H	N
1	CH_3	CH_3	H	135−137[a,b]	$C_{11}H_{15}N_3O$			
					205.26			
2	CH_3	CH_3	Cl	152−154[a]	$C_{11}H_{14}ClN_3O$	55.12	5.89	17.53
					239.71	55.20	6.12	17.64
3	CH_3	$CH(CH_3)_2$	H	73−75	$C_{13}H_{19}N_3O$	66.92	8.21	18.01
				hexane	233.32	67.04	8.30	18.26
4	CH_3	$CH(CH_3)_2$	Cl	113−114	$C_{13}H_{18}ClN_3O$	58.32	6.78	15.69
				hexane	267.76	58.34	6.90	15.73
5	CH_3	$C(CH_3)_3$	H	73−75	$C_{14}H_{21}N_3O$	67.98	8.56	16.99
				hexane	247.34	68.09	8.67	17.07
6		$-(CH_2)_5-$	H	138−140[c]	$C_{14}H_{19}N_3O$			
				50% EtOH	245.32			
7	CH_3	C_6H_5	H	124−125[d]	$C_{16}H_{17}N_3O$			
				50% EtOH	267.33			
8	CH_3	C_6H_5	Cl	123−125	$C_{16}H_{16}ClN_3O$	63.68	5.34	13.92
				50% EtOH	301.78	63.67	5.41	13.86
9	CH_3	C_6H_4-*p*NO_2	H	144−146	$C_{16}H_{16}N_4O_3$	61.53	5.16	17.94
				EtOH	312.33	61.47	5.30	18.02
10	CH_3	C_6H_4-*p*NO_2	Cl	180−182	$C_{16}H_{15}ClN_4O_3$	55.42	4.36	16.16
				EtOH	346.78	55.33	4.48	16.33
11	CH_3	C_6H_4-*p*CF_3	H	175−177[a]	$C_{17}H_{16}F_3N_3O$	60.89	4.89	12.53
					335.33	60.93	5.04	12.59
12	CH_3	C_6H_4-*p*CF_3	Cl	169−171[a]	$C_{17}H_{15}ClF_3N_3O$	55.22	4.09	11.36
					369.78	55.22	4.20	11.45
13	CH_3	C_6H_4-*m*Cl	H	150−151	$C_{16}H_{16}ClN_3O$	63.68	5.34	13.92
				EtOH	301.78	63.68	5.45	13.71
14	CH_3	C_6H_4-*m*Cl	Cl	141−142	$C_{16}H_{15}Cl_2N_3O$	57.16	4.50	12.50
				EtOH	336.22	57.22	4.64	12.67
15	CH_3	C_6H_4-*p*Br	H	138−139[a]	$C_{16}H_{16}BrN_3O$	55.51	4.66	12.14
					346.24	55.80	4.77	12.40
16	CH_3	C_6H_4-*p*Br	Cl	150−151[a]	$C_{16}H_{15}BrClN_3O$	50.48	3.97	11.04
					380.68	50.53	4.13	11.31
17	CH_3	C_6H_4-*p*CH_3	H	104−106[a]	$C_{17}H_{19}N_3O$	72.57	6.81	14.93
					281.36	72.82	6.88	14.86
18	CH_3	C_6H_4-*p*CH_3	Cl	144−146	$C_{17}H_{18}ClN_3O$	64.66	5.75	13.31
				50% EtOH	315.81	64.71	5.80	13.50
19	CH_3	C_6H_4-*p*OCH_3	H	140−142[a]	$C_{17}H_{19}N_3O_2$	68.67	6.44	14.13
					297.36	68.93	6.52	14.37
20	CH_3	C_6H_4-*p*OCH_3	Cl	102−105	$C_{17}H_{18}ClN_3O_2$	61.54	5.47	12.66
				50% EtOH	331.81	61.60	5.63	12.71

[a] Diisopropyl ether:EtOH = 4:1. [b] Literature[5c] mp 128−130 °C. [c] Literature[5c] mp 132−134 °C. [d] Literature[5c] mp 132−134 °C.

Compounds **21** and **22** were prepared in ethanolic solution at room temperature, starting from acetophenone and (*o*-aminobenzoyl)hydrazine or 1-(2′-(methylamino)benzoyl)-1-methylhydrazine, respectively. **21**: mp 171−172 °C (benzene), yield 76%; **22**, mp 97−99 °C (diethyl ether), yield 56%.

Analytical data on 2,2-disubstituted-1,2,3,4-tetrahydro-5*H*-1,3,4-benzotriazepin-5-ones **1**−**20** are shown in Table 5.

Conclusions

(1) The studied 2,2-disubstituted-1,3,4-benzotriazepinones undergo complex molecular rearrangements which involve (i) ring to open-chain tautomerization; (ii) pseudorotation of the ring forms and ring (N-3)-inversion processes; (iii) interconversion of the open-chain forms via *cis*−*trans*-amide bond and/or *Z*/*E* C=N bond isomerizations, with different rates on the NMR time scale, leading to the observation of average and deceptively simple high-resolution ^1H and ^{13}C NMR spectra for most of them in solution at room temperature.

(2) The boat form is the most stable conformation of the ring structures of **1**, **2**, and **7**−**20**, with methyl and phenyl(aryl) groups at C-2, whereas for the sterically congested derivatives **3** and **4**, the inverted boat seems to be the minimum energy conformer from both experimental and PM3 calculations.[6e]

(3) In general, the dynamic processes for **1**−**6** are mainly under thermodynamic control (higher conformational energy differences), while for **7**−**20** lower conformational energy differences between the ring/open and ring/ring forms, and also the higher ring-inversion and (N-3)-inversion energy barriers, make the processes more complex, and they occur under kinetic control.

(4) Larger rotational barrier heights for *cis*−*trans*-amide bond rotation and lower heights for *E*/*Z* C=N bond rotation were found for alkyl-substituted hydrazones of **1**, **3**, and **4** in comparison with their phenyl(aryl) analogues **7**−**20**.

(5) The conjugation and hence the push−pull electronic effects play some role in the barriers to rotation in the open-chain hydrazones of **7**−**20**, but, because of the complexity of the observed rearrangements, their quantitative study in terms of a simple linear correlation: $\log K_x = \rho\sigma^+ + c$, where K_x = [ring]/[chain], was not possible.

Acknowledgment. M.F.S. acknowledges a Fellowship from the Turku University Foundation and in part from the Academy of Finland.

JO962322K